Electrochimica Acta 380 (2021) 138223

Contents lists available at ScienceDirect

Electrochimica Acta

journal homepage: www.elsevier.com/locate/electacta

Enhancement factors in electrochemical surface oxidation enhanced Raman scattering

Sheila Hernandez[a], Juan V. Perales-Rondon[a,b,**], Aranzazu Heras[a], Alvaro Colina[a,*]

[a] Department of Chemistry, Universidad de Burgos, Pza. Misael Bañuelos s/n, E-09001 Burgos, Spain
[b] Department of Analytical Chemistry, Physical Chemistry and Chemical Engineering, University of Alcala. Ctra. Madrid-Barcelona, Km. 33.600, 28871 Alcalá de Henares, Madrid, Spain

ARTICLE INFO

Article history:
Received 18 February 2021
Accepted 20 March 2021
Available online 27 March 2021

Keywords:
Spectroelectrochemistry
Surface enhanced Raman scattering
EC-SERS
Electrochemical surface oxidation enhanced Raman scattering
EC-SOERS

ABSTRACT

Electrochemical Surface Oxidation Enhanced Raman Scattering (EC-SOERS) is a new phenomenon that provokes the enhancement of the Raman signal during the oxidation of a metal surface. Studies carried out so far indicate that carbonyl and carboxyl group are necessary to observe this phenomenon with a delocated charge being an important factor. In this work, the enhancement factors of EC-SOERS for different molecules, which present highly delocated charge and a carboxyl group, have been assessed. The systematic study of the enhancement factors helps to shed more light on the interaction of the molecules with the electrochemically generated SOERS substrates, yielding key information about the properties and specific features of this intriguing phenomenon. For the first time, a systematic information about the enhancement factors of this phenomenon is obtained. Analytical enhancement factors higher than 10^5 are obtained.

1. Introduction

Surface enhanced Raman Scattering (SERS) has become one of the most powerful tools in the field of molecular detection in recent years [1–3]. This technique not only allows the identification of molecules, providing information about the chemical structure, but also gives some insight into the interactions that can take place between the molecule and the nanostructured surface [4–8]. Raman scattering presents some disadvantages such as a weak analytical signal or a low reproducibility on the recorded signals. Many research groups are working hard to achieve higher, more defined and more reproducible Raman signals to better detect different molecules using the SERS phenomenon or other phenomena linked to Raman spectroscopy [9–11].

It is well known that the SERS phenomenon is mainly produced by the combination of two mechanisms [3,12,13]: (1) the electromagnetic mechanism (EM), related to the amplification of the electromagnetic field due to the resonance of surface plasmons at the metallic nanostructured surface (SPR, surface plasmon resonance) and, (2) the chemical mechanism (CM), which is mainly associated with a charge transfer between the molecule and the surface of the substrate. Both mechanisms contribute to enhance the Raman signal. However, while EM-mechanism yields enhancement factors (EFs) between 10^4 and 10^8, the CM-mechanism only shows EFs between 10-10^3 [3,12–14]. The huge Raman amplification achieved in SERS has great implications in different fields such as medicinal chemistry, analytical chemistry, environmental safety, etc [1–3,15].

Recently, our research group discovered a new phenomenon, denoted as EC-SOERS (Electrochemical Surface Oxidation Enhanced Raman Scattering), which enhances the Raman signal during the oxidation of a silver electrode under particular electrolytic conditions [16]. This enhancement is probably related to two main factors: (1) the interaction between the molecule and the silver structures formed during the experiment (Ag/AgCl or Ag^+/AgCl) and (2) the induced adsorption due to the applied potential. These mechanisms are still not clear enough and, therefore, more experiments should be done to understand this new phenomenon.

The goal of this work is to shed more light on the interactions between molecules and silver substrates under particular EC-SOERS conditions. With this objective, a systematic calculation of the EFs for the EC-SOERS phenomenon is made for the first time, providing useful information to better understand this intriguing phenomenon. Assuming that both EM-mechanism and CM-mechanism are involved in EC-SOERS, as described for SERS, it might be possible to determine if any kind of plasmonic species formed during an EC-SOERS experiment are responsible for the enhancement of the Raman signal due to an EM-mechanism

* Corresponding author at: Department of Chemistry, Universidad de Burgos, Pza. Misael Bañuelos s/n, E-09001 Burgos, Spain.
** Corresponding author.
E-mail address: acolina@ubu.es (A. Colina).

https://doi.org/10.1016/j.electacta.2021.138223
0013-4686/

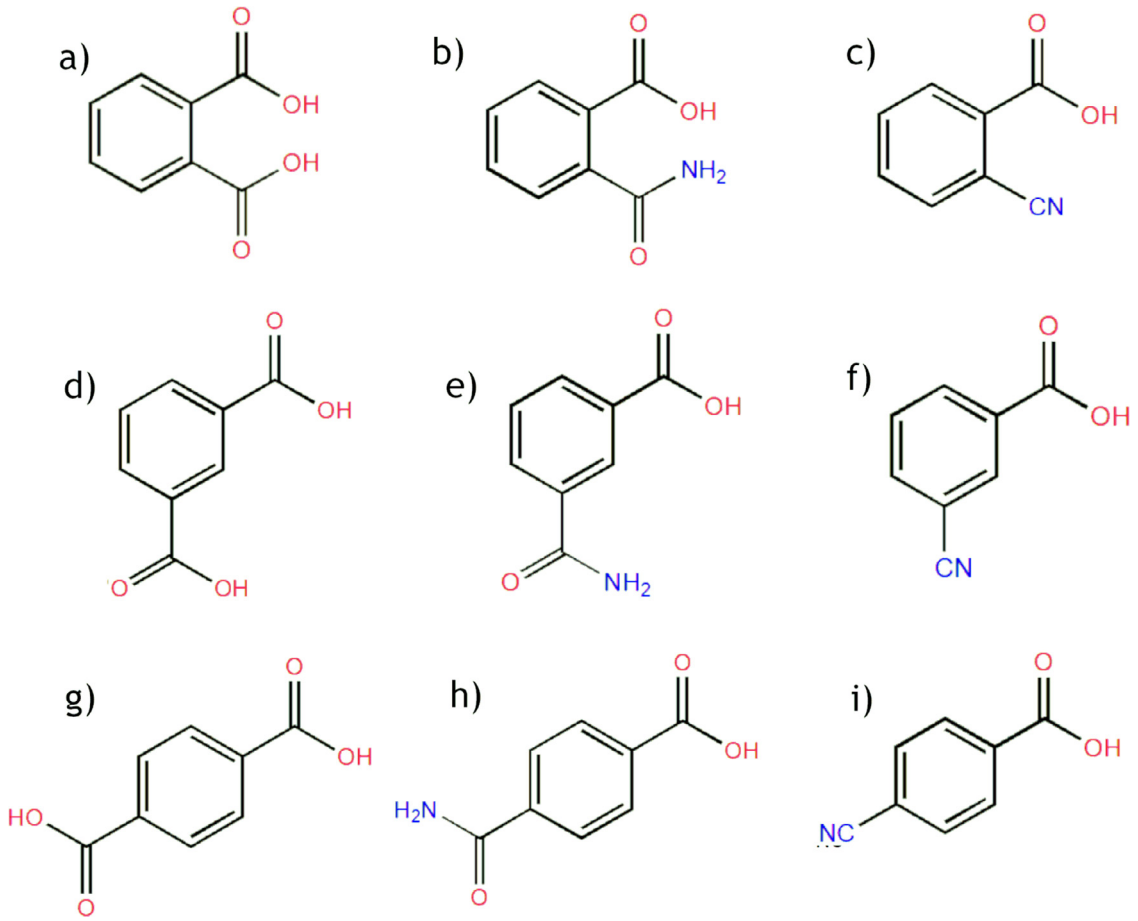

Fig. 1. Structure of the studied molecules: a) phthalic acid (PA), b) phthalamic acid (PAA), c) 2-cyanobenzoic acid (2-CN-BzA), d) isophthalic acid (IPA), e) 3-carboxiamidobenzoic acid (3-CABA), f) 3-cyanobenzoic acid (3-CN-BzA), g) terephthalic acid (TPA), h) terephthalic acid monoamide (TPAM), i) 4-cyanobenzoic acid (4-CN-BzA).

($EF > 10^3$) or, conversely, if that enhancement is only due to a CM-mechanism. It should be emphasized that EFs are strongly dependent on the molecule structure and its interaction with the nanostructured substrate [17–20], mainly linked to the CM-mechanism and the physical or chemical interactions between molecules and metal substrate [3,17] . Thus, different EFs can be obtained for isomers with the same structures [21,22]. It should be also noted that the EM-mechanism will uniformly enhance all the Raman band intensities with the same symmetry, namely, the relative intensities registered by ordinary Raman scattering should not change in SERS and EC-SOERS by this mechanism [3,7,20].

In this work, the effect of changing the functional group as well as its position in different structural isomers in the Raman signal obtained was studied. With this purpose, EFs were calculated for benzene dicarboxylic acid isomers, cyanobenzoic acid isomers, and carboxyamidobenzoic acid isomers (Fig. 1). We have found that all these molecules exhibit a quite good EC-SOERS response, mainly due to the presence of the carboxylic acid group coupled to an aromatic ring. Therefore, a better knowledge on EC-SOERS can be obtained from the systematic analysis of this group of molecules.

Assessment of SERS EF is usually performed using the following equation:

$$EF = \frac{I_{SERS} \cdot N_{Raman}}{I_{Raman} \cdot N_{SERS}} \quad (1)$$

where, I corresponds to the maximum of Raman intensity, for both, ordinary Raman (I_{Raman}) and SERS (I_{SERS}) signals, N_{Raman} is related to the number of molecules contained in the volume of sampled solution whereas N_{SERS} corresponds to the number of molecules adsorbed on the sampled surface [23]. As EC-SOERS is a phenomenon somehow linked to SERS because an enhancement of the Raman signal is provoked, an equation similar to Eq. 1 can be proposed to evaluate the EC-SOERS EF as follow:

$$EF = \frac{I_{SOERS} \cdot N_{Raman}}{I_{Raman} \cdot N_{SOERS}} \quad (2)$$

However, EC-SOERS is a dynamic phenomenon with the electrode surface continuously evolving because the silver surface is being oxidized while an anodic overpotential scan is applied. Consequently, it is quite difficult to calculate the number of molecules adsorbed on the surface of the electrogenerated structures responsible for the EC-SOERS effect. Moreover, it is still unclear what kind of structures induce this phenomenon. Therefore, in this work, instead of calculating the EF, we have selected the analytical enhancement factor (AEF) to evaluate the effect of the molecular structure on the Raman signal enhancement. AEF is also related to the interaction between a molecule and the surface, and it has proven to be a very useful tool to compare the activity of different molecules and the effectiveness of SERS substrates [23–27]. The AEF can be calculated using the following equation:

$$AEF = \frac{I_{SOERS} \cdot C_{Raman}}{I_{Raman} \cdot C_{SOERS}} \quad (3)$$

where, C_{Raman} denotes the concentration of analyte in the solution where the Raman signal (I_{Raman}) is obtained, and C_{SOERS} is the concentration of analyte in the solution where the enhanced Raman signal (I_{SOERS}) is obtained.

Reader should keep in mind that AEF are usually several orders of magnitude lower than EF, because the number of molecules on

the nanostructured surface (N_{SOERS}) is much lower than the number of molecules in all the volume of the solution used (C_{SOERS}) [23]. Therefore, it is expected that the EF of EC-SOERS should be higher than the AEF provided in this work.

The purpose of this work is to obtain a better comprehension of EC-SOERS effect and to understand why some molecules are very sensitive to this phenomenon by the calculation of AEF values.

2. Experimental section

2.1. Reagents and materials

Benzoic acid (BzA, ≥99.5 %, Sigma-Aldrich), phthalamic acid (PAA, 97 %, Sigma-Aldrich), 3-carboxyamidobenzoic acid (3-CABA, Sigma-Aldrich), terephthalic acid monoamide (TPAM, Sigma-Aldrich), 2-cyano-benzoic acid (2-CN-BzA, 94 %, ACROS Organics), 3-cyano-benzoic acid (3-CN-BzA, 98 %, ACROS Organics), 4-cyano-benzoic acid (4-CN-BzA, 99 %, ACROS Organics), phthalic acid (PA, ≥99.5 %, Sigma-Aldrich), isophthalic acid (IPA, 99 %, Sigma-Aldrich), terephthalic acid (TPA, 99+ %, ACROS Organics), perchloric acid ($HClO_4$, 60 %, reagent, Sigma-Aldrich), potassium chloride (KCl, 99+ %, reagent, ACROS Organics). Aqueous solutions were freshly prepared using ultrapure water (18.2 MΩ cm resistivity at 25 °C, Milli-Q Direct 8, Millipore).

2.2. Instrumentation

Time-resolved Raman spectroelectrochemistry (TR-Raman-SEC) and Raman spectroscopy experiments were carried out using a customized SPELEC-Raman (DRP-SPELECRAMAN, Metrohm-DropSens), which integrates a spectrophotometer, a laser source of 785 nm and a bipotentiostat/galvanostat. Silver screen-printed electrodes (Ag-SPE, DRP-C013, Metrohm-DropSens) and a customized Raman-SEC cell are used to ensure a good reproducibility of the experiments. These electrodes consist of a silver working electrode of 1.6 mm diameter, a counter electrode made of carbon and silver paint as pseudo-reference, all of them printed in a ceramic platform. The power of the laser was 80 mW (254 mW/cm^2) and the integration time was kept 1 s for all experiments.

2.3. Time-resolved Raman spectroelectrochemistry experiments

The electrochemical technique selected for Raman-SEC experiments was cyclic voltammetry, and all Raman spectra were registered simultaneously with the electrochemical response. Before each experiment, a pretreatment of the electrode is made to ensure the reproducibility. It consists of 2 potential cycles between the vertex potentials of +0.40 V and -0.40 V, starting at -0.025 V in anodic direction at 0.02 V s^{-1}, using a solution containing 0.1 M $HClO_4$ + 0.005 M KCl ($HClO_4$/KCl medium). After this pretreatment, the solution is removed, adding the test solution that contains the target molecule in the same supporting electrolyte medium ($HClO_4$/KCl medium). These Raman-SEC experiments are carried out using the same electrochemical protocol and recording Raman spectra every second (integration time = 1 s). For a better comparison, all EC-SOERS spectra shown below correspond to those obtained at the maximum of Raman signal (see asterisk, in Fig. 2), which is obtained between +0.40 and +0.27 V in the cathodic direction during the second cycle of the SEC experiment.

3. Results and discussion

3.1. Analysis of the electrochemical responses

Fig. 2 shows the cyclic voltammograms (CVs) obtained during EC-SOERS experiments in comparison with the EC-SOERS response for the main band of each molecule. The electrochemical responses show a very similar behavior regardless of the studied molecule. Thus, the current is mainly related to the oxidation and reduction of the silver electrode surface in this medium [16,28] and it is not due to the electrochemical transformation of the molecules studied. First, an anodic peak around +0.02 V is observed related to oxidation of Ag and the generation of AgCl due to the presence of chloride ions from the supporting electrolyte. This process occurs until a high anodic current evolves at potentials higher than +0.30 V, related to massive electrogeneration of Ag^+ in solution. In the backward scan, around +0.30 V, free silver cations are reduced to Ag while a second cathodic peak evolves approximately at -0.10 V related to the reduction of AgCl to Ag and the generation of silver nanostructures on the electrode surface [16,28].

Despite these similarities, which can be observed in all CVs shown in Fig. 2, there are some details that can be related to the adsorption of the target molecule. The maximum current observed during the massive oxidation of the silver electrode, to form Ag^+ at potentials higher than +0.30 V, slightly changes depending on the strength of adsorption of the molecule. For example, for the three dicarboxylic acids (PA, IPA and TPA) the lowest current is achieved for *ortho*-isomer (Fig. 2A) and the highest for the *para*-isomer (Fig. 2G) which can be related to a stronger adsorption for PA than IPA and TPA. Similar results have been obtained with the other two family of structural isomers shown in Fig. 2. Therefore, the adsorption of molecules of the same family to the silver electrode depends on the position of the substituent, which affect the enhancement of the Raman signal of the isomers, as will be discussed below.

There are also some differences in the spectroscopic response. As can be seen in the voltaRamangrams in Fig. 2, the maximum of the Raman signal is not obtained at the same potential. For *ortho*-isomers, this maximum is reached at a lower anodic potential value, which also could indicate a stronger interaction with the substrate, whereas for *meta*- and *para*- isomers the maximum of Raman signal is found at higher anodic potentials (near +0.40 V), and the signal decays before than the one for *ortho*- isomers. It is noteworthy that other Raman bands of these molecules have the same behavior than the Raman band selected and shown in Fig. 2. The Raman spectra registered at this maximum, labeled with an asterisk (*) in Fig. 2, are shown in Fig. 3. These spectra will then be used to make a comparison within the group of molecules tested in this work and will serve to calculate the corresponding AEF.

3.2. Comparison between the Raman and EC-SOERS spectra

The spectrum of a molecule in solution obtained in a simple Raman experiment presents some important differences with the corresponding EC-SOERS spectrum. The shape of the spectrum as well as the relative intensities of the bands provide key information about the interaction between the substrate and a specific molecule [3,20]. For that reason, a rational comparison between the Raman spectra in solution and the corresponding EC-SOERS spectra obtained in a TR-Raman-SEC experiment was performed for all molecules. It is worth noting that a high concentration of the target molecule in solution is needed to obtain measurable bands in the Raman spectra (0.20 M PA, 0.15 M IPA, 0.20 M TPA, 0.90 M PAA, 0.80 M 3-CABA, 0.80 M TPAM, 0.76 M 2-CN-BzA, 0.76 M 3-CN-BzA and 0.75 M 4-CN-BzA). These spectra were obtained in a solution without performing any SEC experiment and with an integration time of 1 s. On the other hand, EC-SOERS spectra were taken during the corresponding TR-Raman-SEC experiment. To properly compare the signals, representative bands were selected, and the ratio between these bands was calculated to study the relative change of the heights of different bands.

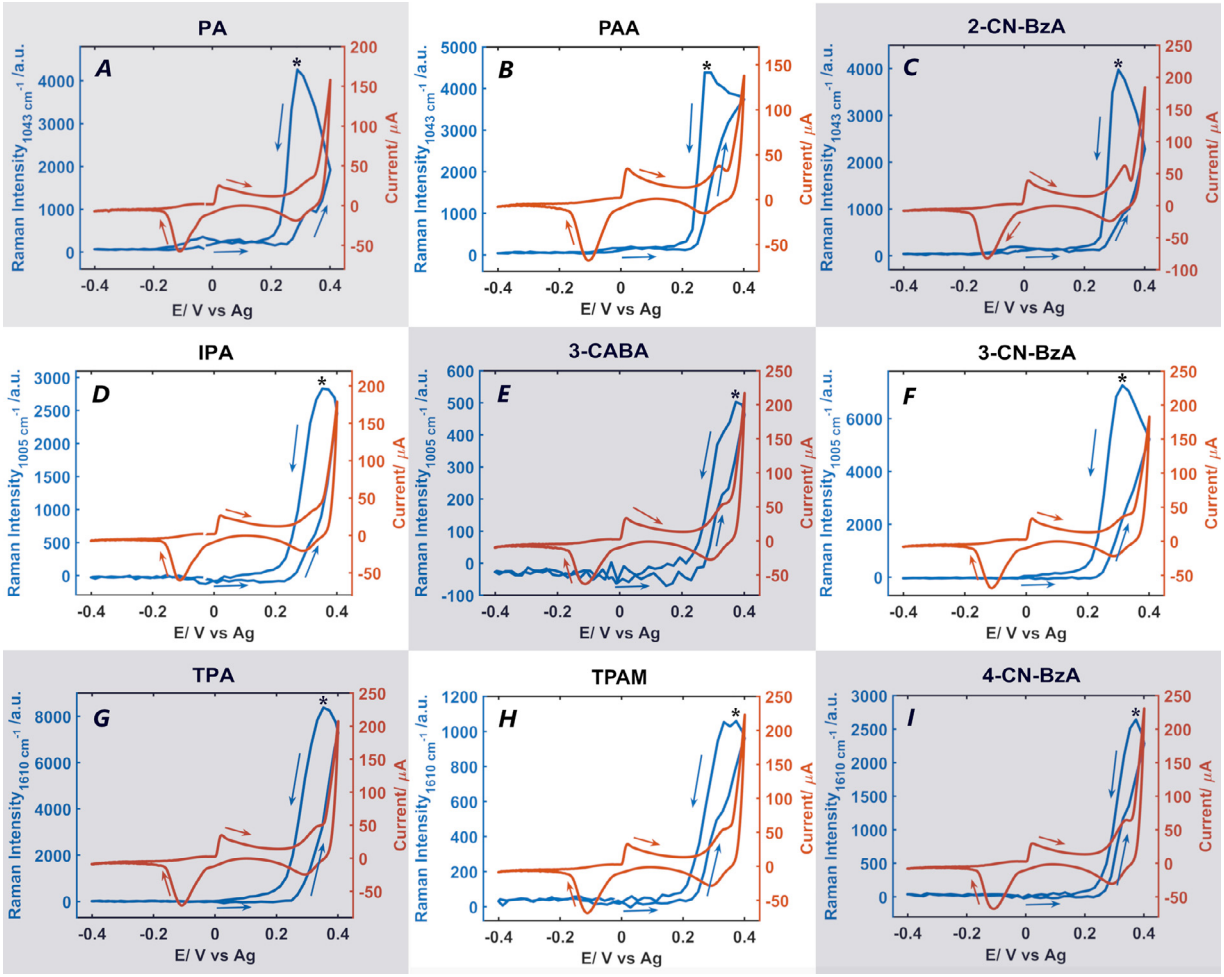

Fig. 2. Comparison between CVs (orange curves) and the evolution of the EC-SOERS response for the main band of each molecule with the potential applied (VoltaRamangram, blue curves), for the different studied molecules: A) 0.1 mM phthalic acid (PA), B) 1 mM phthalamic acid (PAA), C) 0.2 mM 2-cyano-benoic acid (2-CN-BzA), D) 0.1 mM isophthalic acid (IPA), E) 0.1 mM 3-carboxyamidobenzoic acid (3-CABA), F) 0.2 mM 3-cyano-benzoic acid (3-CN-BzA), G) 0.1 mM terephthalic acid (TPA), H) 0.1 mM terephthalic acid monoamide (TPAM), I) 0.02 mM 4-cyano-benzoic acid (4-CN-BzA). All of them were prepared in $HClO_4$/KCl medium. The CVs were performed at 0.02 V s^{-1} between -0.40 V and +0.40 V, starting at -0.025 V in the anodic direction. The asterisk (*) marks for each molecule the potential corresponding to the Raman spectra shown in Fig. 3, which are used to calculate the AEFs.

Bands assignment are shown in Tables S1, S2 and S3 in the supplementary materials document (SM). In order to calculate the ratio, the spectra were normalized to the main band of the studied molecule. Thus, for *ortho*-isomers, the band related with ν_{18a} (C-C vibrations) peaking at 1043 cm^{-1} was selected [5,29,30]; for *meta*-isomers, band peaking at 1005 cm^{-1}, which is related to ν_{12} vibration mode (C-C-C trigonal bending) [31,32]; and, finally, for *para*-isomers the band peaking around 1610 cm^{-1} was chosen associated with ν_{8a} (C-C stretching) [31–33]. Values corresponding to the ratio of Raman/EC-SOERS intensity are shown in the Table S4 in the SM.

Fig. 3 shows the normalized Raman and EC-SOERS spectra for the different target molecules. Relative intensities of the bands provide interesting information about the behavior of the spectra for these molecules, which can be summarized as follow:

1) For *ortho*-isomers (Fig. 3A, 3B and 3C) some differences between Raman and EC-SOERS spectra can be observed. The most significant difference between the spectra is appreciated for the vibration modes corresponding to the carboxyl groups, $\delta(COO^-)$ and $\nu(COO^-)$. On the one hand, $\delta(COO^-)$ yields a much higher value (in terms of $I_{Raman}/I_{Raman\ at\ 1043\ cm\text{-}1}$) in EC-SOERS than in Raman. On the other hand, $\nu(COO^-)$ is more intense in Raman than in EC-SOERS. From this result, we conclude that the orientation of the molecule and the orientation of the functional groups interacting with the substrate is a fundamental aspect to consider, as is usually observed in SERS [5,8,20]. A higher ratio for $\delta(COO^-)$ in EC-SOERS suggests that the interaction of the molecule with the EC-SOERS substrate is taking place by one of the oxygen atoms in the carbonyl group [34].

Other interesting bands are those corresponding to C-C stretching (ν_{8a} and ν_{8b}), at 1580 cm^{-1} and 1602 cm^{-1}, respectively. These bands present different relative intensities depending on the experiment. EC-SOERS shows a higher enhancement of the band at 1585 cm^{-1}. On the contrary, the Raman spectrum presents a higher signal of the band at 1600 cm^{-1}. These modes of vibration are highly related to the symmetry of the molecule. Therefore, the difference in the response demonstrates a change in the symmetry of the molecule as a result of the interactions with the EC-SOERS substrate. Assuming a chemical interaction of the molecules with the substrate, a charge transfer mechanism could be expected, which explains the higher AEF of the $\delta(COO^-)$ vibration mode (see Table 1) for *ortho*-isomers. It should be noted that, as has been stated above from the CVs (Fig. 2), *ortho*-isomers shows a higher adsorption to the silver electrode than the other isomers in the family, yielding a higher Raman signal.

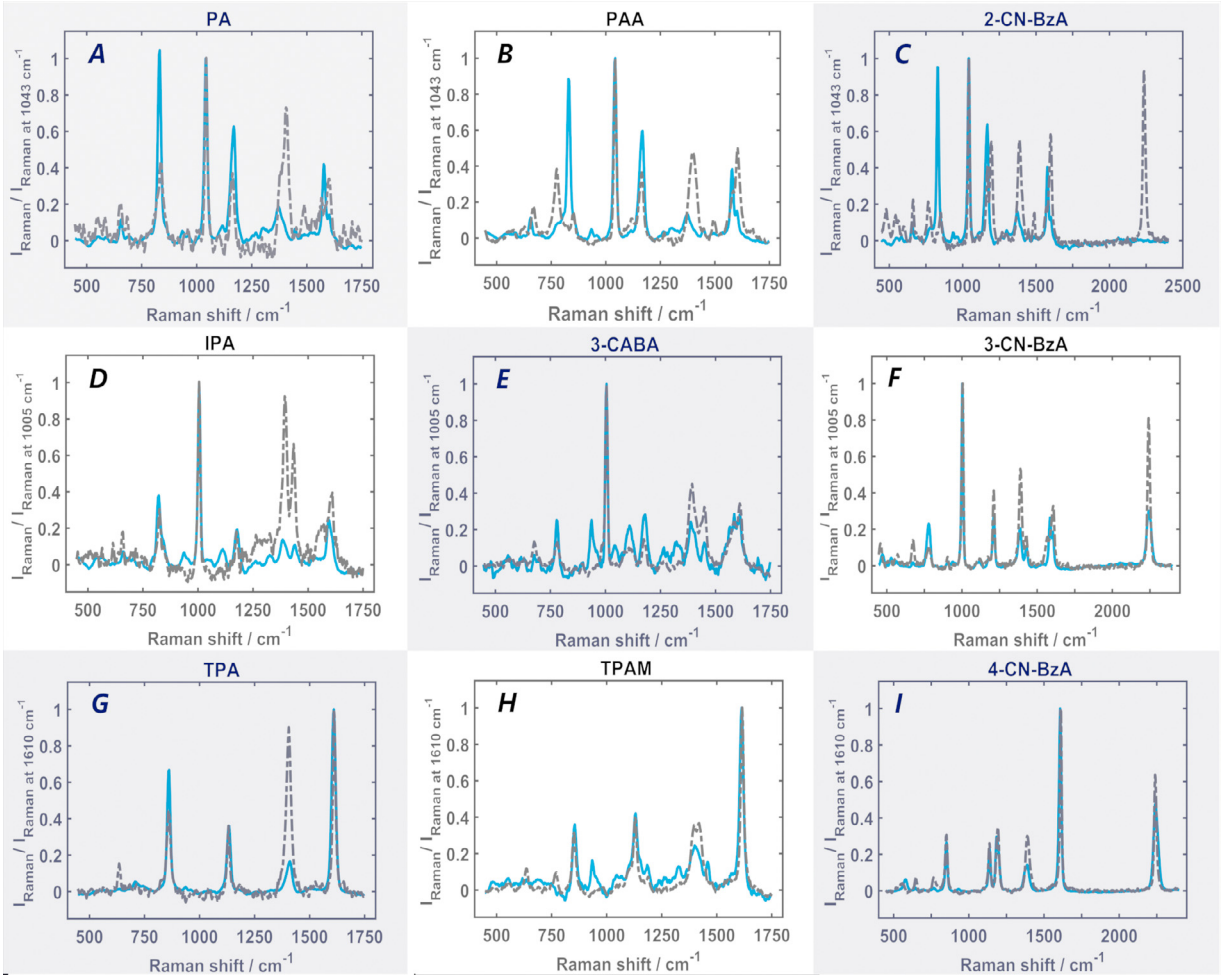

Fig. 3. Normalized Raman spectrum (grey dotted line) and normalized EC-SOERS spectrum (blue solid line) for: A) phthalic acid (PA), B) phthalamic acid (PTA), C) 2-cyano-benzoic acid (2-CN-BzA), D) isophthalic acid (IPA), E) 3-carboxyamidobenzoic acid (3-CABA), F) 3-cyano-benzoic acid (3-CN-BzA), G) terephthalic acid (TPA), H) terephthalic acid monoamide (TPAM), I) 4-cyano-benzoic acid (4-CN-BzA). Raman spectra were registered in 0.1 M NaOH medium and EC-SOERS spectra were registered at the maximum Raman intensity, marked with an asterisk (*) in Fig. 2, during a TR-Raman-SEC experiment. The experimental conditions are the same described in Fig 2.

2) In the case of the *meta*-isomers (Fig. 3D, 3E and 3F) changes for the vibration modes corresponding to the carboxyl groups ($\delta(COO^-)$ at 778-822 cm^{-1} and $\nu_S(COO^-)$ around 1385 cm^{-1}) are less noticeable. Therefore, a weaker interaction of these molecules with the substrate, as well as a weaker interaction through the oxygen atom of the carboxyl group must be assumed. Additionally, the inversion in the relative intensities of $\delta(COO^-)$ and $\nu_S(COO^-)$ between Raman and EC-SOERS spectra can be also observed for the three molecules. For instance, $\delta(COO^-)$ is more intense in EC-SOERS spectra while $\nu_S(COO^-)$ vibration mode is higher in Raman spectra. In this group of molecules, the inversion is more pronounced in IPA, probably due to the presence of two carboxyl groups which would confirm that these groups are those that interact with the EC-SOERS substrate. Therefore, the interaction of the carboxyl groups with the EC-SOERS substrate is an important factor to explain the enhancement of the Raman signal, as will be shown in the following section. In this case, the two functional groups in the molecules are electron acceptors and a competition between them can be expected because of their position in the molecules. Electron acceptor groups in *ortho*- and *para*- have a different influence on the polarizability of the molecule and the vibration of the ring than *meta*-isomers.
3) Two different behaviours are observed in the case of the *para*-isomers. The first one is related to the cyano- and amide- benzoic derivatives, yielding small differences between Raman and EC-SOERS spectra. Therefore, for these two molecules the effect of an EM-mechanism could be more important than that of the CM-mechanism [20]. Without a clear understanding of the structures responsible of the EC-SOERS, it is very difficult to estimate how much the substrate structure-molecule interaction might affect the enhancement of the Raman signal. However, the magnitude of the AEF for these isomers should be useful to explain the role of CM-mechanism and EM-mechanism in the enhancement. Thus, AEF higher than 10^5 should be related to an important effect of an EM-mechanism [13]. On the other side, the spectral behaviour observed in TPA that contains two carboxyl groups is markedly different from the other two *para*-isomers. In this case, the two-carboxyl groups are far enough away in the structure of the molecule to allow both to interact with the substrate. For this molecule, the relative intensities related to the two vibration modes ascribed to carboxyl groups are sharply different in a normal Raman measurement and during an EC-SOERS experiment. Namely, $\delta(COO^-)$ band has a relative intensity of 0.7 for EC-SOERS *vs.* 0.4 for Raman, and $\nu(COO^-)$ band has a relative intensity of 0.9 for Raman *vs.* 0.2 for EC-SOERS (see table S4). Once again, the relative intensities suggest that TPA is mostly interacting with the EC-SOERS substrate through one of the oxygen atoms of their carboxylates.

Table 1
AEFs for molecules in Fig. 1 and for all vibration modes of each molecule. EC-SOERS measurements were taken at the asterisk (*) marked in Fig. 2 correspondig to the spectra shown in Fig. 3, which are used to calculate the AEF. All AEFs are calculated using Eq. 3.

PA		PTA		2-CN-BzA	
Raman shift / cm^{-1}	AEF	Raman shift / cm^{-1}	AEF	Raman shift / cm^{-1}	AEF
655	$4.1{\cdot}10^4$	655	$6.9{\cdot}10^3$	655	$1.8{\cdot}10^4$
832	$1.7{\cdot}10^5$	832	$6.9{\cdot}10^4$	832	$2.5{\cdot}10^5$
1043	$7.0{\cdot}10^4$	1043	$1.1{\cdot}10^4$	1043	$4.1{\cdot}10^4$
1165	$1.2{\cdot}10^5$	1165	$1.8{\cdot}10^4$	1165	$6.4{\cdot}10^4$
1370	$1.8{\cdot}10^4$	1370	$3.1{\cdot}10^3$	1370	$1.1{\cdot}10^4$
1580	$1.8{\cdot}10^5$	1580	$1.7{\cdot}10^4$	1580	$9.0{\cdot}10^4$
1602	$2.5{\cdot}10^4$	1602	$3.4{\cdot}10^3$	1602	$9.2{\cdot}10^3$
IPA		3-CABA		3-CN-BzA	
Raman shift / cm^{-1}	AEF	Raman shift / cm^{-1}	AEF	Raman shift / cm^{-1}	AEF
822	$5.2{\cdot}10^4$	782	$1.8{\cdot}10^4$	778	$1.2{\cdot}10^5$
1005	$2.7{\cdot}10^4$	1005	$9.4{\cdot}10^3$	1005	$5.6{\cdot}10^4$
1175	$6.1{\cdot}10^4$	1178	$1.7{\cdot}10^4$	1211	$3.7{\cdot}10^4$
1385	$4.7{\cdot}10^3$	1388	$4.8{\cdot}10^3$	1385	$2.2{\cdot}10^4$
1440	$5.4{\cdot}10^3$	1449	$2.8{\cdot}10^3$	1429	$3.3{\cdot}10^4$
1594	$2.3{\cdot}10^4$	1585	$9.1{\cdot}10^3$	1585	$9.3{\cdot}10^4$
-	-	1610	$7.2{\cdot}10^3$	1605	$3.2{\cdot}10^4$
				2244	$2.0{\cdot}10^4$
TPA		TPAM		4-CN-BzA	
Raman shift / cm^{-1}	AEF	Raman shift / cm^{-1}	AEF	Raman shift / cm^{-1}	AEF
862	$1.3{\cdot}10^5$	855	$1.2{\cdot}10^4$	852	$1.0{\cdot}10^5$
1134	$8.5{\cdot}10^4$	1131	$1.2{\cdot}10^4$	1138	$1.2{\cdot}10^5$
		1184	$1.9{\cdot}10^4$	1184	$1.2{\cdot}10^5$
1411	$1.5{\cdot}10^4$	1405	$7.1{\cdot}10^3$	1388	$7.1{\cdot}10^4$
1611	$8.3{\cdot}10^4$	1613	$1.1{\cdot}10^4$	1607	$1.3{\cdot}10^5$
				2241	$8.5{\cdot}10^4$

As can be observed in the spectra of the molecules (Fig. 3) Raman and EC-SOERS spectra show big differences with respect to the relative intensities of the bands. However, the differences in the Raman shift of these bands are small. It should be noted that Raman spectra were taken in 0.1 M NaOH solutions (due to the low solubility of these molecules, which is highly improved in this medium), and therefore, molecules were deprotonated. The coincidence of the bands for Raman and EC-SOERS spectra, although the pH is so different (pH=1 for EC-SOERS experiments and pH=13 for Raman measurements), suggests that a deprotonation of the acid forms of these molecules occurs during their interaction with the EC-SOERS substrate as a result of the applied potential [35].

Focusing the attention onto EC-SOERS spectra, two bands related to protonated/deprotonated species can be analyzed, namely, the $\delta(COO^-)$ at 832 cm^{-1} and the ν(C-COOH) at 800 cm^{-1}. These bands are the best indicative of the protonation state of carboxyl group. Ma and Harris [35] demonstrated that when positive potentials are applied, the pKa changes and the deprotonated form can be the predominant even at pH as acid as 1. In our case, an oxidative deprotonation can be expected from the bands in the spectra, with the carboxylate being attracted by the EC-SOERS substrate.

3.3. Analysis of the analytical enhancement factors

The intrinsic dynamic character of the electrochemistry experiments, together with the oxidation of the silver surface, makes extremely difficult to calculate the surface coverage of a molecule at a specific time, because both the whole surface and the molecules interacting with the new substrate are constantly changing with the applied potential. Therefore, as was stated above, EC-SOERS enhancement factor cannot be assessed as indicated in Eq. 2. Nevertheless, EC-SOERS analytical enhancement factor , which is very useful to compare the different responses from the analytes, as long as the rest of the conditions remain the same, is much easier to calculate according to Eq. 3. With the aim of calculating the AEF, the Raman signal was registered in a concentrated alkaline solution of the specific molecule (between 0.20-0.90 M, exact concentrations indicated above) and it is compared with the EC-SOERS response of a diluted solution in $HClO_4$/KCl medium at a potential where the Raman signal is enhanced. Table 1 shows the AEFs for all molecules in Fig. 1 and for different vibration modes of each molecule. It is noteworthy that AEFs were obtained from results that present high reproducibility with %RSD lower than 10 % in most of cases and lower than 20 % for all of them, which ensure that the conclusions extracted from these results are reliable. Additionally, this low dispersion makes EC-SOERS a good candidate to perform analytical measurements, as has been previously demonstrated [36,37].

The EC-SOERS spectra corresponding to PA, PTA and 2-CN-BzA (Fig. 4) are very similar, which would indicate that the interaction with the substrate is also similar. According to these spectra and the results discussed in the previous sections, it can be concluded that the carboxyl group and the aromatic ring are those that mainly interact with the EC-SOERS substrate. The absence of the characteristic bands at 2244 cm^{-1} of -CN group in 2-CN-BzA, which is present in solution in ordinary Raman (Fig. 3C), and of any characteristic bands of $-CONH_2$ in PAA can be related to two different facts. The first one is a steric hindrance, due to the proximity of two functional groups. The second one is that the position of the molecules on the EC-SOERS surface provokes this vibration to be forbidden by the surface selections rules [38,39].

It should be noted that AEFs help to understand the interaction of the molecules with the substrate. The highest AEFs of PA, PTA and 2-CNBzA were calculated for the band assigned to the symmetric scissoring of COO^- around 832 cm^{-1}, Table 1, indicating that the carboxyl group is interacting with EC-SOERS substrate. Raman signals corresponding to vibrations of the aromatic ring (breathing, CH bending and CC bending) are also enhanced. These results confirm the proposed interaction of the molecules with the EC-SOERS substrate.

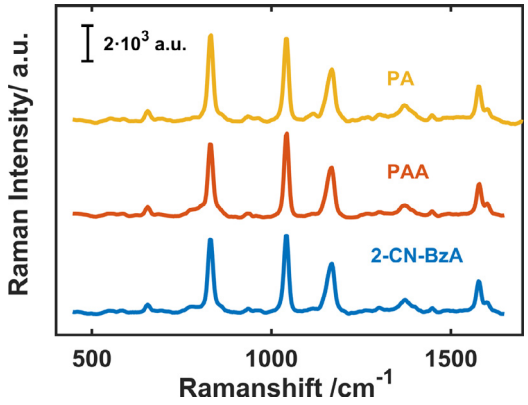

Fig. 4. EC-SOERS spectra of 0.1 mM phthalic acid (PA, yellow line), 1 mM phthalamic acid (PAA, orange line) and 0.2 mM 2-cyanobenzoic acid (2-CN-BzA, blue line) in 0.1 M $HClO_4$ and 0.005 M KCl as electrolytic medium. Spectra selected were collected during TR-Raman-SEC experiments, choosing the spectra where the maximum Raman intensity is reached (points marked as *, in Fig. 2). Integration time was 1 s.

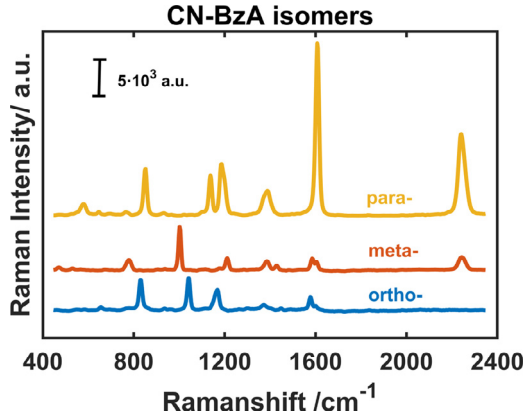

Fig. 5. EC-SOERS spectra of 0.2 mM 2-cyanobenzoic acid (blue line), 0.2 mM 3-cyanobenzoic acid (orange line) and 0.2 mM 4-cyanobenzoic acid (yellow line). All of them were collected during a TR-Raman-SEC experiment (at the maximum of Raman signal, see asterisks (*) in Fig. 2, and at an integration time of 1s. The electrolytic medium was 0.1 M $HClO_4$ and 0.005 M KCl.

Another interesting comparison is the one corresponding to the three *cyano*-isomers, which provides information about the effect of the substituent's position (Fig. 5). At first glance, it could be deduced that 4-CN-BzA is the isomer with the best interaction with the substrate; however, the highest response for 4-CN-BzA can be related to the intrinsic Raman cross section of this molecule, since the same trend can be observed in Raman spectra (data not shown). When the comparison is made in terms of AEF values, the best response is not straightforward because different bands should be compared. For example, in the case of the $\delta(COO^-)$ vibration, the best AEF value is found for 2-CN-BzA ($2.5{\cdot}10^5$). However, if the asymmetric stretching of COO^- is selected for the comparison, the highest AEF value is found for 4-CN-BzA ($7.1{\cdot}10^4$). Furthermore, *meta*- and *para*-isomers show similar AEF for δ(COO-) and ν(CN), indicating that these molecules are parallel to the surface, which amplifies the two vibration modes in the same way.

3.4. Influence of the substituent group

The comparison of EC-SOERS spectra can be also made in terms of the functional groups in the studied molecules. In this case, dicarboxylic and cyano-benzoic acid isomers present higher AEF values than carboxamide benzoic acid isomers, and all of them present higher AEF values than benzoic acid (BzA) (see Table S5). The behavior of BzA in EC-SOERS is also shown in the SM (Fig. S1), where can be seen the CV in comparison with the voltaRamangram at 1005 cm^{-1} (Fig. S1A) and the comparison between the Raman and EC-SOERS spectrum for this molecule (Fig. S1B). The three substituent groups (-COOH, -CN and -$CONH_2$) are electron acceptor by resonance effect, making the aromatic ring poorer in electrons than benzoic acid. The electron acceptor effect follows the trend -CN group > -COOH group > -$CONH_2$ group, which agrees with the AEF values obtained for the studied molecules.

Clearly, in all cases, cyano-isomers present higher AEF values, which can be explained in terms of resonance in aromatic rings, where -CN is a strong electron acceptor and withdraw charge easily compared to -$CONH_2$ or -COOH groups.

Finally, further investigations should be made to shed more light on this phenomenon, which has not been yet fully explained; however, the results presented here provide high-quality information to understand deeply the phenomenon.

4. Conclusions

For the first time, a systematic analysis of the analytical enhancement factors for EC-SOERS is reported. For all the studied molecules, EC-SOERS spectra are in a good agreement with ordinary Raman spectra.

There is a significant influence of the substituent group, showing higher AEF values for molecules with higher electron acceptor character groups, such as -CN and -COOH groups, whereas -$CONH_2$ group yields lower AEF values. The position of the functional group also presents an important influence, with the *ortho*- and *para*- positions presenting the higher AEF. The interaction of the molecules with the silver substrate seems to be a key factor in EC-SOERS AEFs, as is observed in SERS, suggesting that a CM-mechanism could present a higher influence in the enhancement of the *ortho*-isomers whereas an EM-mechanism could be more important for *para*-isomers.

AEF values are usually lower than EF values, therefore, EF in EC-SOERS should be greater than those reported in this work. Nevertheless, AEF values higher than 10^5 have been observed, which suggests that both mechanism (EM-mechanism and CM-mechanism) are implied in this phenomenon, as it happens in SERS. The presence of the EM-mechanism indicates that some kind of plasmonic structure is being generated during the oxidation of the silver substrate.

More experiments and theoretical studies should be done to clarify several aspects related to the EC-SOERS phenomenon. Even so, this work is a first step that suggests that silver structures with plasmonic properties could be generated at an oxidation process, being related to this phenomenon.

Declaration of Competing Interest

The authors declare that they have no known competing financial interests or personal relationships that could have appeared to influence the work reported in this paper.

Acknowledgments

Authors acknowledge the financial support from Ministerio de Economía, y Competitividad (Grant CTQ2017-83935-R-AEI/FEDERUE), Junta de Castilla y León (Grant BU297P18) and Ministerio de Ciencia, Innovación y Universidades (Grant RED2018-102412-T). J.V.P-R. thanks Junta de Castilla y León for his postdoctoral fellowship (Grant BU033-U16). S.H. thanks Junta de Castilla y León and European Social Fund for her predoctoral fellowship. William Cheuquepan and Martin Perez-Estebanez are acknowl-

edged for the fruitful discussions on the manuscript. Jorge Gonzalez is acknowledged for his help in the laboratory.

Author Contribution

S.H and J.P-R. contributed to the acquisition of data. S.H., J.P-R., A.H and A.C. contributed to the conception, design and implementation of the research and to the analysis and interpretation of the results. All the authors contributed to the writing of the manuscript and to the revision of the manuscript critically for important intellectual content. This work has been headed by J.P-R and A.C.

Supplementary materials

Supplementary material associated with this article can be found, in the online version, at doi:10.1016/j.electacta.2021.138223.

References

[1] D. Graham, M. Moskovits, Z.-Q. Tian, SERS – facts, figures and the future, Chem. Soc. Rev. 46 (2017) 3864–3865, doi:10.1039/C7CS90060K.
[2] B. Sharma, R.R. Frontiera, A.-I. Henry, E. Ringe, R.P. Van Duyne, SERS: Materials, applications, and the future, Mater. Today 15 (2012) 16–25, doi:10.1016/S1369-7021(12)70017-2.
[3] J. Langer, D. Jimenez de Aberasturi, J. Aizpurua, R.A. Alvarez-Puebla, B. Auguié, J.J. Baumberg, G.C. Bazan, S.E.J. Bell, A. Boisen, A.G. Brolo, J. Choo, D. Cialla-May, V. Deckert, L. Fabris, K. Faulds, F.J. García de Abajo, R. Goodacre, D. Graham, A.J. Haes, C.L. Haynes, C. Huck, T. Itoh, M. Käll, J. Kneipp, N.A. Kotov, H. Kuang, E.C. Le Ru, H.K. Lee, J.-F. Li, X.Y. Ling, S.A. Maier, T. Mayerhöfer, M. Moskovits, K. Murakoshi, J.-M. Nam, S. Nie, Y. Ozaki, I. Pastoriza-Santos, J. Perez-Juste, J. Popp, A. Pucci, S. Reich, B. Ren, G.C. Schatz, T. Shegai, S. Schlücker, L.-L. Tay, K.G. Thomas, Z.-Q. Tian, R.P. Van Duyne, T. Vo-Dinh, Y. Wang, K.A. Willets, C. Xu, H. Xu, Y. Xu, Y.S. Yamamoto, B. Zhao, L.M. Liz-Marzán, Present and Future of Surface-Enhanced Raman Scattering, ACS Nano 14 (2020) 28–117, doi:10.1021/acsnano.9b04224.
[4] D. Ibañez, A. Santidrian, A. Heras, M. Kalbáč, A. Colina, Study of adenine and guanine oxidation mechanism by surface-enhanced Raman spectroelectrochemistry, J. Phys. Chem. C. 119 (2015) 8191–8198, doi:10.1021/acs.jpcc.5b00938.
[5] N. Piergies, E. Proniewicz, Y. Ozaki, Y. Kim, L.M. Proniewicz, Influence of substituent type and position on the adsorption mechanism of phenylboronic acids: Infrared, raman, and surface-enhanced raman spectroscopy studies, J. Phys. Chem. A. 117 (2013) 5693–5705, doi:10.1021/jp404184x.
[6] J.L. Castro, M.R. Lopez-Ramirez, J.F. Arenas, J. Soto, J.C. Otero, Evidence of deprotonation of aromatic acids and amides adsorbed on silver colloids by surface-enhanced raman scattering, Langmuir 28 (2012) 8926–8932, doi:10.1021/la204702w.
[7] M.R. Lopez-Ramirez, C. Ruano, J.L. Castro, J.F. Arenas, J. Soto, J.C. Otero, Surface-enhanced Raman scattering of benzoate anion adsorbed on silver nanoclusters: Evidence of the transient formation of the radical dianion, J. Phys. Chem. C. 114 (2010) 7666–7672, doi:10.1021/jp911865w.
[8] Z.Q. Tian, B. Ren, Adsorption and reaction at electrochemical interfaces as probed by surface-enhanced Raman spectroscopy, Annu. Rev. Phys. Chem. 55 (2004) 197–229, doi:10.1146/annurev.physchem.54.011002.103833.
[9] L. Jensen, C.M. Aikens, G.C. Schatz, Electronic structure methods for studying surface-enhanced Raman scattering, Chem. Soc. Rev. 37 (2008) 1061–1073, doi:10.1039/b706023h.
[10] S.-Y. Ding, J. Yi, J.-F. Li, B. Ren, D.-Y. Wu, R. Panneerselvam, Z.-Q. Tian, Nanostructure-based plasmon-enhanced Raman spectroscopy for surface analysis of materials, Nat. Rev. Mater. 1 (2016) 16021, doi:10.1038/natrevmats.2016.21.
[11] A. Balčytis, Y. Nishijima, S. Krishnamoorthy, A. Kuchmizhak, P.R. Stoddart, R. Petruškevičius, S. Juodkazis, From fundamental toward applied SERS: shared principles and divergent approaches, Adv. Opt. Mater. 6 (2018) 1–29, doi:10.1002/adom.201800292.
[12] S. Schlücker, Surface-enhanced raman spectroscopy: concepts and chemical applications, Angew. Chemie Int. Ed. 53 (2014) 4756–4795, doi:10.1002/anie.201205748.
[13] P.L. Stiles, J.A. Dieringer, N.C. Shah, R.P. Van Duyne, Surface-enhanced raman spectroscopy, Annu. Rev. Anal. Chem. 1 (2008) 601–626, doi:10.1146/annurev.anchem.1.031207.112814.
[14] N. Valley, N. Greeneltch, R.P. Van Duyne, G.C. Schatz, A look at the origin and magnitude of the chemical contribution to the enhancement mechanism of surface-enhanced Raman spectroscopy (SERS): theory and experiment, J. Phys. Chem. Lett. 4 (2013) 2599–2604, doi:10.1021/jz4012383.
[15] M. Fan, G.F.S. Andrade, A.G. Brolo, A review on recent advances in the applications of surface-enhanced Raman scattering in analytical chemistry, Anal. Chim. Acta 1097 (2020) 1–29, doi:10.1016/j.aca.2019.11.049.
[16] J.V. Perales-Rondon, S. Hernandez, D. Martin-Yerga, P. Fanjul-Bolado, A. Heras, A. Colina, Electrochemical surface oxidation enhanced Raman scattering, Electrochim. Acta 282 (2018) 377–383, doi:10.1016/j.electacta.2018.06.079.
[17] J. Cabalo, J.A. Guicheteau, S. Christesen, Toward understanding the influence of intermolecular interactions and molecular orientation on the chemical enhancement of SERS, J. Phys. Chem. A. 117 (2013) 9028–9038, doi:10.1021/jp403458k.
[18] S.L. Kleinman, B. Sharma, M.G. Blaber, A.I. Henry, N. Valley, R.G. Freeman, M.J. Natan, G.C. Schatz, R.P. Van Duyne, Structure enhancement factor relationships in single gold nanoantennas by surface-enhanced raman excitation spectroscopy, J. Am. Chem. Soc. 135 (2013) 301–308, doi:10.1021/ja309300d.
[19] M.V. Cañamares, J.V. Garcia-Ramos, S. Sanchez-Cortes, M. Castillejo, M. Oujja, Comparative SERS effectiveness of silver nanoparticles prepared by different methods: A study of the enhancement factor and the interfacial properties, J. Colloid Interface Sci. 326 (2008) 103–109, doi:10.1016/j.jcis.2008.06.052.
[20] A.G. Brolo, D.E. Irish, B.D. Smith, Applications of surface enhanced Raman scattering to the study of metal-adsorbate interactions, J. Mol. Struct. 405 (1997) 29–44, doi:10.1016/S0022-2860(96)09426-4.
[21] N.S. Chong, K. Donthula, R.A. Davies, W.H. Ilsley, B.G. Ooi, Significance of chemical enhancement effects in surface-enhanced Raman scattering (SERS) signals of aniline and aminobiphenyl isomers, Vib. Spectrosc. 81 (2015) 22–31, doi:10.1016/j.vibspec.2015.09.002.
[22] K.L. Posey, M.G. Viegas, A.J. Boucher, C. Wang, K.R. Stambaugh, M.M. Smith, B.G. Carpenter, B.L. Bridges, S.E. Baker, D.A. Perry, Surface-enhanced vibrational and TPD study of nitroaniline isomers, J. Phys. Chem. C. 111 (2007) 12352–12360, doi:10.1021/jp071833f.
[23] E.C. Le Ru, E. Blackie, M. Meyer, P.G. Etchegoint, Surface enhanced raman scattering enhancement factors: a comprehensive study, J. Phys. Chem. C. 111 (2007) 13794–13803, doi:10.1021/jp0687908.
[24] S. Ben-Jaber, W.J. Peveler, R. Quesada-Cabrera, C.W.O. Sol, I. Papakonstantinou, I.P. Parkin, Sensitive and specific detection of explosives in solution and vapour by surface-enhanced Raman spectroscopy on silver nanocubes, Nanoscale 9 (2017) 16459–16466, doi:10.1039/c7nr05057g.
[25] X. Sun, N. Wang, H. Li, Deep etched porous Si decorated with Au nanoparticles for surface-enhanced Raman spectroscopy (SERS), Appl. Surf. Sci. 284 (2013) 549–555, doi:10.1016/j.apsusc.2013.07.132.
[26] S. Hong, X. Li, Optimal size of gold nanoparticles for surface-enhanced Raman spectroscopy under different conditions, J. Nanomater. 2013 (2013) 790323, doi:10.1155/2013/790323.
[27] L. He, M. Lin, H. Li, N.J. Kim, Surface-enhanced Raman spectroscopy coupled with dendritic silver nanosubstrate for detection of restricted antibiotics, J. Raman Spectrosc. 41 (2010) 739–744, doi:10.1002/jrs.2505.
[28] J.V. Perales-Rondon, S. Hernandez, A. Heras, A. Colina, Effect of chloride and pH on the electrochemical surface oxidation enhanced Raman scattering, Appl. Surf. Sci. 473 (2019) 366–372, doi:10.1016/j.apsusc.2018.12.148.
[29] J. Gao, Y. Hu, S. Li, Y. Zhang, X. Chen, Adsorption of benzoic acid, phthalic acid on gold substrates studied by surface-enhanced Raman scattering spectroscopy and density functional theory calculations, Spectrochim. Acta - Part A Mol. Biomol. Spectrosc. 104 (2013) 41–47, doi:10.1016/j.saa.2012.11.103.
[30] S.W. Joo, S.W. Han, H.S. Han, K. Kim, Adsorption and stability of phthalic acid on a colloidal silver surface: surface-enhanced Raman scattering study, J. Raman Spectrosc. 31 (2000) 145–150, doi:10.1002/(SICI)1097-4555(200003)31:3⟨145::AID-JRS506⟩3.0.CO;2-1.
[31] J.F. Arenas, J.I. Marcos, Infrared and Raman spectra of phtalate, isophtalate and terephtalate ions, Spectrochim. Acta Part A Mol. Spectrosc. 35 (1979) 355–363, doi:10.1016/0584-8539(79)80191-9.
[32] D.A. Perry, J.S. Cordova, W.D. Spencer, L.G. Smith, A.S. Biris, SERS, SEIRA, TPD, and DFT study of cyanobenzoic acid isomer film growth on silver nanostructured films and powder, J. Phys. Chem. C. 114 (2010) 14953–14961, doi:10.1021/jp104256h.
[33] S.H. Kim, S.J. Ahn, K. Kim, Vibrational spectroscopic study of 4-cyanobenzoic acid adsorbed on silver, J. Phys. Chem. 100 (1996) 7174–7180, doi:10.1021/jp953309r.
[34] J.S. Suh, J. Kim, Three distinct geometries of surface-adsorbed carboxylate groups, J. Raman Spectrosc. 29 (1998) 143–148, doi:10.1002/(sici)1097-4555(199802)29:2⟨143::aid-jrs204⟩3.0.co;2-23.
[35] C. Ma, J.M. Harris, Surface-enhanced raman spectroscopy investigation of the potential-dependent acid-base chemistry of silver-immobilized 2-mercaptobenzoic acid, Langmuir 27 (2011) 3527–3533, doi:10.1021/la1044859.
[36] S. Hernandez, J.V. Perales-Rondon, A. Heras, A. Colina, Determination of uric acid in synthetic urine by using electrochemical surface oxidation enhanced Raman scattering, Anal. Chim. Acta 1085 (2019) 61–67, doi:10.1016/j.aca.2019.07.057.
[37] S. Hernandez, J.V. Perales-Rondon, A. Heras, A. Colina, Electrochemical SERS and SOERS in a single experiment: a new methodology for quantitative analysis, Electrochim. Acta 334 (2020) 135561, doi:10.1016/j.electacta.2019.135561.
[38] M. Moskovits, Surface selection rules, J. Chem. Phys. 77 (1982) 4408–4416, doi:10.1063/1.444442.
[39] M. Moskovits, J.S. Suh, Surface selection rules for surface-enhanced Raman spectroscopy: calculations and application to the surface-enhanced Raman spectrum of phthalazine on silver, J. Phys. Chem. 88 (1984) 5526–5530, doi:10.1021/j150667a013.